

# Estimation of flow velocity in open channels with the use of electromagnetic flowmeter and neural network

**Abstract.** Presented paper describes signal processing for electromagnetic flow meter dedicated for open channels. The investigation on the possibilities to use a multilayer neural network in the estimation of the flow velocity is discussed with respect to the distortions caused by the measuring method and external noises.

**Streszczenie.** Referat prezentuje problematykę przetwarzania w algorytmie pomiarowym przepływomierza elektromagnetycznego dla kanału otwartego. Przedstawiono w nim wyniki badań nad możliwością wykorzystania sieci neuronowej typu perceptron wielowarstwowy w wyznaczaniu prędkości przepływu cieczy w warunkach zniekształceń sygnału wnoszonych przez metodę oraz zakłócenia zewnętrzne. (Pomiar przepływu wody w kanale otwartym przy wykorzystaniu metody elektromagnetycznej i sieci neuronowej)

**Keywords:** electromagnetic flowmeter, application of neural networks.

**Słowa kluczowe:** przepływomierz elektromagnetyczny, zastosowania sieci neuronowych.

## Introduction

Electromagnetic flowmeters play an important role in many industrial and environmental applications because of their unquestionable advantages. First of all the method can handle the flow measurements even when the filing of the channels varies. Besides, it allows working where there is vegetation in water including shallow water with very low velocities. Thanks to that the method suits the flow measurements in open channels, appears to be very useful for scientists dealing with hydrological models to quantify how land development and sources of pollutions affects the aquatic ecosystems and helps to control irrigation channels. All that is possible thanks to the relatively simple principle of operation based on the Faraday's law that incorporates no moving parts in practical equipment and excludes the needs of periodic maintenance. The sensor is simply composed of two electrodes dipped in conductive and moving liquid that can be treated as a conductor examined in the presence of magnetic field that must be excited. The primary parameter  $V$  – the velocity flow can thus be obtained by measurements of voltage  $U$  induced on the electrodes as it is described by the product of the velocity, the magnetic induction  $B$  existing in the measuring area and the distance between electrodes  $D$ :

$$(1) \quad U = V \cdot B \cdot D$$

Unfortunately, the voltage is highly distorted by external disturbances that hinder the information about flow velocity. Their spectrum is generally very broad but the dominant component is of low frequency, very close to DC. The component is mainly brought about by the differences between the electrochemical potentials of the liquid and the material of the electrodes. The resulting interference voltages fluctuate and can exceed the amplitudes of the induced flow signals by several thousands of times. In such conditions the measurement with DC excitation yielding a DC voltage modulated by the flow velocity is practically impossible. To handle the measurements, the energy of the magnetic field used by the sensor is usually switched to offer flat segments of the waveforms when simple measuring algorithms can be adopted [1]. However, the algorithms are not too accurate – typically 5-10% because despite the presence of external disturbances, the switching field itself incorporates additional distortions to the output signal. The sources of the distortions can be recognized as the errors of the method. The first source is connected with the inertial reaction of the current responsible for the field.

The reaction is caused by the finite bandwidth of the power amplifier loaded with the coil inductance. Besides, the switching field involves the so called "transformer effect". The source of the effect is the loop formed by the electrodes and a conduction path across the liquid. The loop and the coil constitute the secondary and primary turns of a hypothetic transformer and gives rise to additional flow-like signals that increase with the excitation frequency and change in time as the electrical contact over the electrode-liquid interfaces also changes. Because of that the switching frequency usually doesn't exceed several hertz. Otherwise the switching edges can be strong enough to even saturate the preamplifier connected to the electrodes. And eventually, the need to reduce the effects of the external disturbances brings about the necessity to use high pass filters to block the components. The filters incorporate additional modification of the measuring signal especially when its frequency is also low. Besides, there is an inevitable presence of the 50/60Hz line interferences that affect the signals.

The modifications of the output signal by the above phenomena are depicted in Fig.1 where an exemplary rectangular voltage excitation of frequency 5Hz was used.

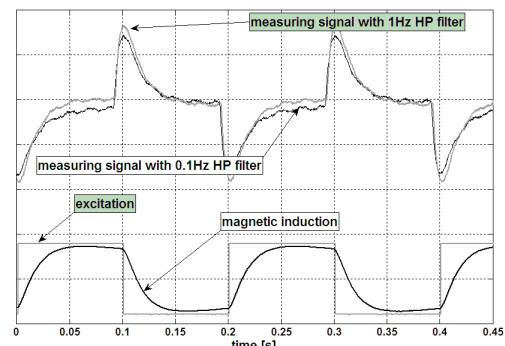


Fig.1. From excitation to the output measuring signal – distortions involved by the method

As it can be seen, the segments of the magnetic field that do not induce any voltage by the transformer effect and where the magnitude of the signal is strictly proportional to the velocity  $V$  are very narrow. The paper discusses a new exploratory or data mining approach that can be seen as an alternative to the classical algorithms. The approach gives no peculiar attention to all the phenomena behind the waveform of the measuring signal. In particular, it doesn't look for any flat segments of the magnetic field. The

approach is based on finding an appropriate group of signal parameters in order to establish a quantitative relationship between them and the response – the real flow velocity. Such relationship determines the grounds for the assessment of the flowmeter from the metrological point of view as it allows predicting the values of the response when only the output signal is currently known. The quality of the relationship depends on both the parameters and the technique to build the model and should be considered in the terms of the generalization ability. In other words, there should a data pool to build the model and another data pool to assess its quality. In the paper the mapping from the flow signals to the real velocities was carried out with the use of ordinary approach based on the multiple linear regression (MLR) and with the use of a multilayer neural network as well. As a measure of the model's performance, the common *MSE* value was used:

$$(2) \quad MSE = \frac{1}{M} \sum_{i=1}^M (d_i - d_{io})^2,$$

where  $M$  is the number of samples used in the assessment,  $d_i$  is the desired value (destination) and  $d_{io}$  is the output of the model.

### Experimental setup

The base for any exploratory data analysis is the access to real experimental data. Besides, any transducer can be always seen as a combination of software and hardware. For the needs of the paper the data was obtained with the use of a laboratory set. The set enables making measurements in the conditions of real flows existing in open channels and is depicted in Fig. 2.

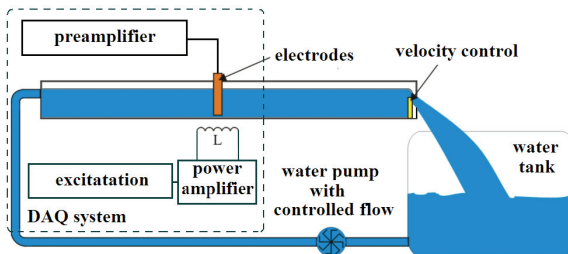


Fig. 2. Experimental setup of the laboratory model

The main component of the set is a 3m long and 12cm wide channel made of PVC supplied with a water pump of regulated volumetric flow. The electrodes are made of stainless steel and can be placed parallel to magnetic field lines with the use of a dedicated holder. The holder also enables to make a compact connection between the electrodes and the conditioning preamplifier. To control the flow velocity a set of 9 little sluices changing the cross section of the channel can be adopted. In the conditions of constant volumetric flow the sluices offer 9 corresponding flow velocities. Thanks to that there is the possibility to obtain various combinations of velocities  $V$  and heights of filling  $H$  of the channel simply by changing the volumetric flow and the sluices. The magnetic field inside the measurement area is excited by a coil  $L$  of impedance  $10\Omega$  in series with  $250\text{mH}$ . Data acquisition and excitation is conducted by the same Agilent U2542 ADC/DAC system controlled by Matlab environment.

During the experiments performed for the needs of the paper, the measured magnetic field peak with the use of rectangular voltage excitation and the power amplifier was  $1\text{mT}$ . In the conditions of available flow velocities, the field

yielded the levels of the signal below merely  $100\mu\text{V}$  whereas all the external disturbances remained unchanged. Because of that the signal acquired by the ADC converter was first processed by the preamplifier designed and built to increase signal to noise ratio. The basic circuit of the preamplifier is depicted in Fig. 3. As the signal comes from two not grounded and not isolated electrodes (there must be a good contact with water), the best way to suppress common-mode signals is to use one of commercially available instrumentation amplifiers with high common-mode rejection ratio. Because of relatively low output impedance of the electrodes immersed in water, the amplifier with low input voltage noise spectral density is desired at the same time. Such noise is offered by amplifiers with bipolar transistor input stages. Eventually, the AD8221 integrated instrumentation amplifier was used with its  $120\text{dB}$  of CMRR for the first, second and third line harmonics and with  $8\text{nV}/\text{Hz}^{1/2}$  of noise density [2]. The circuit uses the standalone three-op-amp topology with a unity gain difference amplifier in the output stage where the total amplification is set by one external resistor  $R_G$ . The problem of the DC-like external and differential disturbances is usually solved by capacitors constituting the AC-coupling of the inputs. But in the case of flow signals such solution is impermissible as it could considerably degrade the CMRR because of lack of perfect symmetry of the capacitors. To condition the small flow signals in the presence of large low frequency components a simple additional circuit was adopted with the use of OPA2132 forming an active external feedback as depicted in Fig. 3.

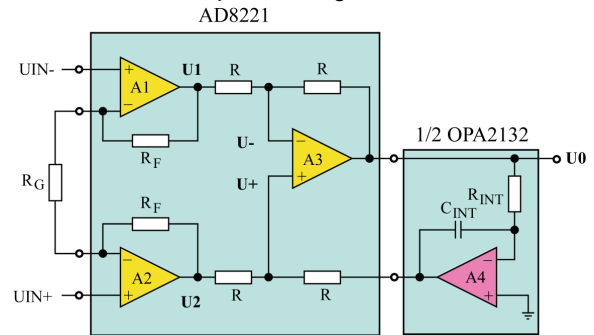


Fig. 3. The basic circuit of the preamplifier to condition the flow signals

The operational amplifier A4 integrates the output of the instrumentation amplifier and puts the resulting signal back to the non-inverted input of the built-in differential amplifier A3. Thanks to that any presence of a DC at the output of the instrumentation amplifier causes a negative linear increase in the output voltage of the A4 that zeros the origin. According to the theory of feedback, the integrator can be seen as a transmittance:

$$(3) \quad \gamma = \frac{1}{j\omega R_{INT} \cdot C_{INT}}.$$

The potentials of the A3 input terminals are then determined by the transmittance and the resistor dividers:

$$(4) \quad U_- = \frac{U_1}{2} + \frac{U_0}{2}, \quad U_+ = \frac{U_2}{2} - \frac{U_0}{2} \cdot \gamma$$

According to the assumptions behind the operational amplifier, the potentials must be identical. Equating both expressions in (4) and solving for  $U_0/(U_2-U_1)$  yields the closed loop amplification of the output stage – equation (5). The fraction describes the transmittance of a high-pass filter

whose corner 3dB frequency is  $f_c=1/(2\pi R_{INT}C_{INT})$ . So setting the values of  $R_{INT}$  and  $C_{INT}$  there is the possibility to control the filtration of low frequency components without degrading the CMRR.

$$(5) \quad K_{C-L} = \frac{U_0}{U_2 - U_1} = \frac{j\omega R_{INT} C_{INT}}{1 + j\omega R_{INT} C_{INT}}$$

Care must be taken as a high value of the corner frequency that is desired with respect to DC removal can disable the possibilities to use classical algorithms at the same time – see Fig. 1. According to the scope of the paper, the frequency is however set to relatively high value of 1Hz that causes error magnitude 2% at 5Hz. The value reduces the influence of the low frequency disturbances efficiently and the estimation of the flow velocity in the conditions of the resulting distorted output signals is carried out by the proposed algorithm.

### Data pool and preprocessing

The data pool for numerical experiments was collected in the laboratory set and includes output waveforms acquired for three volumetric flows. The flows were measured by finding the durations needed to fill a container of known volume. The statistics of such measurements are presented in Table 1.

Table 1. Results of the flow measurements with the 99% conf.level

estimate of the flow [cm <sup>3</sup> /s]	extended uncertainty [cm <sup>3</sup> /s]
246	±3
499	±4
820	±8

With the use of the flows together with the sluices there were 27 different flow velocities in that way. The acquisition process was designed to provide 200 output signals of duration 1s for each of the velocities. In order to examine the generalization ability, the data pool was divided into the learning set containing data for 21 velocities (about 78%) and the testing set containing signals for the rest 6 velocities (about 22%).

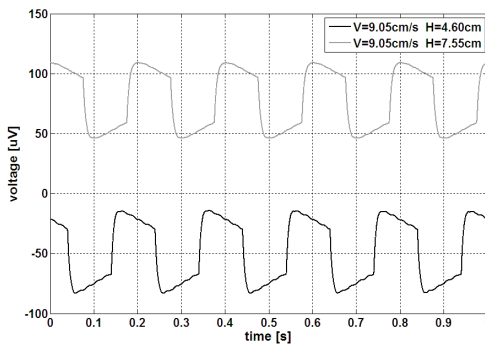


Fig. 4. Averaged flow signals corresponding to the same flow velocity that occurred at two different fillings of the channel (the DCs were artificially added for the presentation purposes)

As the base for generating signal parameters  $x_i$  needed for prediction, the primary and secondary representations of the signal – the time waveform and its Fourier transform were explored. In order to carry out the initial assessment of the flow signals, an additional experiment was established to acquire two waveforms corresponding to the same flow velocity and two different fillings of the channel. With the use of averaging performed over 200 realizations, two

signals depicted in Fig. 4 were taken into further consideration. Since the filling changes the level and shape of the output signal as expected because of the transformer effect, in the case of the primary representation the parameters often used in statistical signal processing and electrical engineering were adopted as potential predictors. They were: waveform factor, kurtosis and inter-quartile range. The waveform factor is commonly used in describing the shape of AC signals. In the case of rectangular waveform with 50% duty factor, the value of the waveform factor equals 1. The kurtosis and inter-quartile range are basic descriptive statistics measuring the shape and dispersion of the data distribution, respectively. Two exemplary experimental data distributions – histograms of signals presented in Fig. 4 are depicted in Fig. 5 and 6 for the comparison purposes.

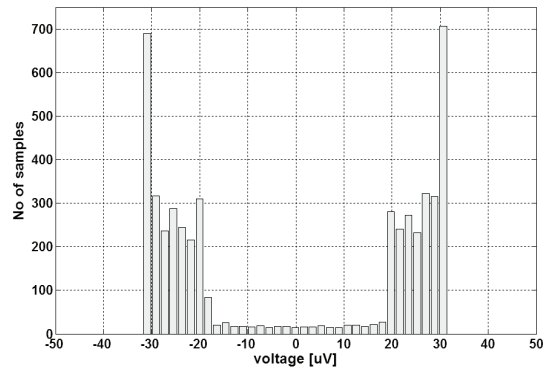


Fig. 5. Exemplary empirical distributions of signal samples when  $V=9.05\text{cm/s}$  and  $H=4.60\text{cm}$

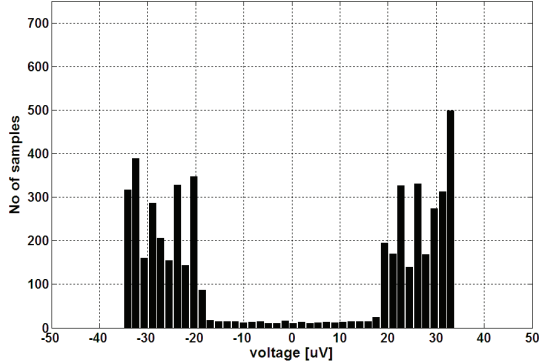


Fig. 6. Exemplary empirical distributions of signal samples when  $V=9.05\text{cm/s}$  and  $H=7.55\text{cm}$

Despite the same velocities, the distributions and the waveforms differ and the difference can be quantitatively expressed to some extent by vectors of the above three parameters. The signal acquired at the lower filling has a bit narrower tails of the distribution and is described by the vector [1.03 1.17 51.73] whereas the signal acquired at the higher filling has longer rise time and is described by the vector [1.04 1.21 54.24].

To fill up the description of the signals by more parameters, the secondary representation – the magnitude of the Fourier transform was also explored. The differences visible in waveforms and distributions exist also in the frequency domain as depicted in Fig. 7 and 8, where spectra of signals corresponding to the same flow velocity are presented. As the Fourier spectrum compresses the information about signals because its ability to concentrate energy in smaller areas in the frequency domain, the first 100 lines of it were taken as features describing a flow signal. To further explore the spectral data and describe it

with fewer quantities, the ordinary descriptive statistics for the spectrum samples were calculated.

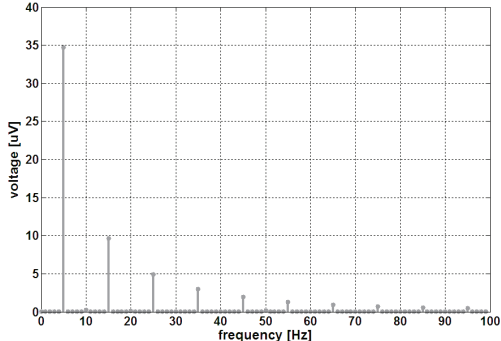


Fig. 7. Spectrum of the exemplary flow signal when  $V=9.05\text{cm/s}$  and  $H=4.60\text{cm}$

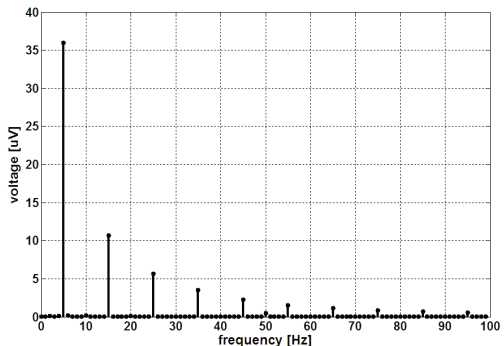


Fig. 8. Spectrum of the exemplary flow signal when  $V=9.05\text{cm/s}$  and  $H=7.55\text{cm}$

The concept of spectral moments was also adopted [4]. The concept assumes that the given spectrum describes the probability density function of a random variable. Such a distribution can be characterized by moments just like expected value, variance etc. With the use of the spectrum and integration, the parameters can be computed directly from definitions.

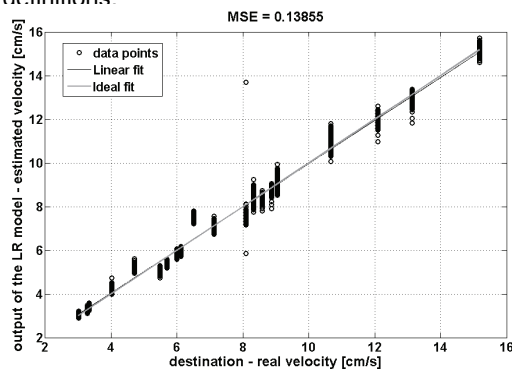


Fig. 9. Input-output characteristic of the flowmeter based on interquartile range as a single predictor (results for the learning data)

In this way a large vector of 112 features coming from the primary and secondary representations of flow signals arose. However, none of the parameters alone can be used to build the input-output characteristic of the flowmeter because of poor performance of the linear regression (LR) – see Fig. 9, where the process of fitting the linear model to data described by one of the parameters – the inter-quartile range is presented. As it can be seen, many data points are far away from the ideal linear fit. The values of the  $MSE$  for other selected parameters are presented in the Table 2.

Table 2. The quality of linear fitting for selected parameters  $x_i$

$x_i$	1 <sup>st</sup> spectral moment	2 <sup>nd</sup> spectral moment	1 <sup>st</sup> spectral line	2 <sup>nd</sup> spectral line
$MSE$	1.15	1.71	0.21	1.77

To find better results simultaneous using of the above parameters is necessary. However, such large sets of possible predictors are usually redundant because of correlation causing problems with the generalization ability. As has been proved in [5], to acquire this ability, the regression model should possess as low number of weights as needed to reduce the error function. Thanks to that the model is forced to reveal the statistical characteristics of the data rather than the individual patterns. So the last step of preprocessing is to convert the set of variables into a new one with reduced dimension and preserved information needed to build the model. One of the approaches is to perform the principal component analysis (PCA) of the matrix composed of the rows containing vectors of raw parameters and then use the resulting principal components as regressors on the vector of real velocities. The approach is sometimes called principal component regression.

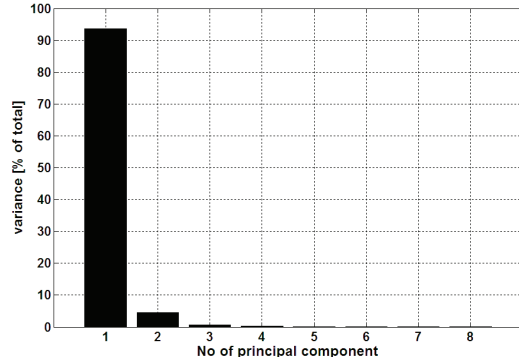


Fig. 10. Variances explained by the first 8 principal components

The orthogonality of the principal components eliminates the correlation problem whereas the reduction of the dimensionality is usually done by keeping only a few of the first components with the largest variances that explain the matrix of original predictors. The distribution of variances for the first several principal components extracted from the learning set is depicted in Fig. 10. As it can be seen, the first component by itself explains about 93% of the variance and taking into account eight components provides over 99%. So the initial set of 112 predictors can be efficiently reduced to a final set much less numerous.

### Building the model

Two alternative techniques were examined to relationship between final predictor variables discussed above and the real flow velocity: multiple linear regression methodology (MLR) and multilayer perceptron (MLP). In the case of MLR, only a strictly linear additive model without any interaction and quadratic terms was used:

$$(6) \quad V = w_0 + w_1 x_1 + w_2 x_2 + \dots + w_N x_N + \varepsilon$$

The model is described by weights  $w_i$  and incorporates random error  $\varepsilon$  whose norm is minimized in the estimation process of the weights. The results of modeling with respect to the generalization ability (the use of testing data) are depicted on correlation plots in Fig. 11 and 12. The number of predictors after PCA was selected experimentally to 8 to achieve low values of  $MSE$ . Using the set of predictors has decreased the  $MSE$  value as compared to the results

presented in Fig. 9 and in the Table 2, where only single predictors were used.

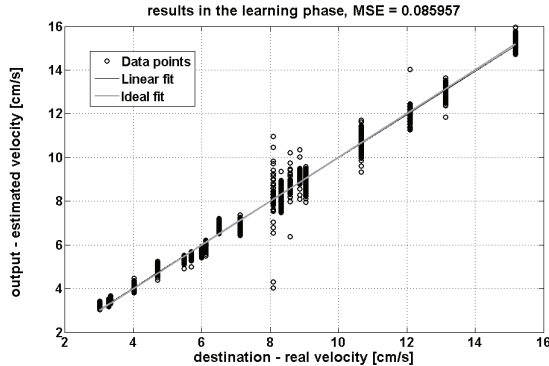


Fig.11. Correlation between outputs of the MLR model and real flow velocities in the learning phase

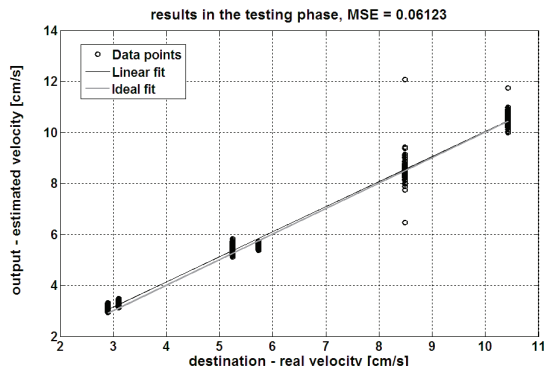


Fig.12. Correlation between outputs of the MLR model and real flow velocities for the data not exposed in the learning phase

In the case of MLP network a structure with one hidden layer containing 6 neurons was chosen. All neurons in the hidden layer are characterized by the sigmoidal activation functions whereas the function for the one output neuron is obviously linear.

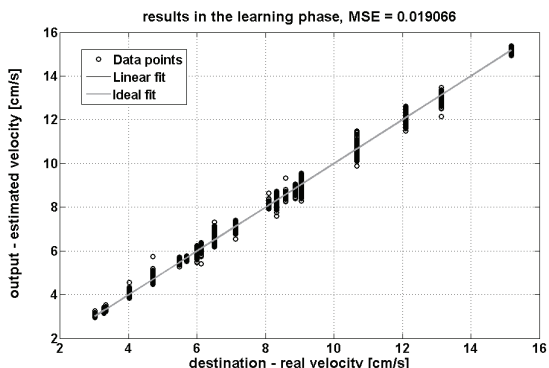


Fig.13. Correlation between outputs of the neural MLP model and real flow velocities in the learning phase

As the MLP network is capable to approximate any multidimensional data with arbitrary accuracy obtained by increasing the number of neurons, its quality must be assessed by results obtained when the weights are frozen after finishing the learning phase and when the testing data are processed. The results obtained in the learning phase are depicted in Fig. 13 whereas the results of prediction for the data that were not exposed to the network to find its weights are depicted in Fig. 14. Similarly to the MLR model - the number of features obtained after PCA as well as the structure of the network have been found experimentally to achieve low MSE values in both phases.

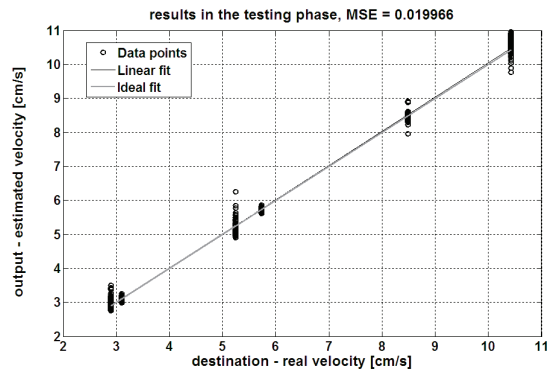


Fig.14. Correlation between outputs of the neural MLP model and real flow velocities for the data not exposed in the learning phase

It is worth to note that the model based on MLP network further improve the input-output characteristic of the flowmeter as compared to the MLR model and models based on single predictors. The lower *MSE* values in learning and testing transpose to better linearity and suppression of disturbances.

## Conclusions

The paper has presented the method of exploratory characterization of signals available in the electromagnetic method of flow measurement in open channels. The waveforms, empirical distributions and Fourier spectra have provided the set of features well suited for the prediction task. The set of 8 different features based on principal component analysis has been worked out to predict the flow velocity. They have formed the input vector to the ordinary multiple regression model and to neural MLP universal approximator, responsible for the final prediction. Application of the neural network has enhanced the performance of the flowmeter as compared to the model established by the linear regression. The numerical experiments performed on the real flow signals, have proved good prediction rates of the proposed combination of the presented hardware with its filtration ability and the MLP neural network. The average relative bias of prediction on the testing data not taking part in the learning process was 1% and the average relative standard uncertainty was 2%. The values seem to be satisfactory from the practical point of view.

## REFERENCES

- [1] Bonfig K., New developments in magnetic flow measurement in partly filled open channels, *Proceeding of IMEKO Congress*, 1982, pp. 131-139.
- [2] AD8221 data sheet available at [www.analog.com](http://www.analog.com).
- [3] Kugelstadt T., Getting the most out of your instrumentation amplifier design, *Analog Applications Journal - Texas Instruments Incorporated*, 4Q 2005, available at [www.ti.com/aaaj](http://www.ti.com/aaaj).
- [4] Vuskovic M., Du S., Spectral Moments for Feature Extraction from Temporal Signals, *Int. Journal of Information Technology*, vol. 11, No 10, 2005, pp. 112-122.
- [5] Hornik K., Stinchcombe M., White H., Multilayer feedforward networks are universal approximators, *Neural Networks*, vol. 2, pp. 359 – 366, 1989.

*Authors:* prof. dr hab. inż. Andrzej Michalski, Politechnika Warszawska, Instytut Elektrotechniki Teoretycznej i Systemów Informacyjno Pomiarowych, ul. Plac Politechniki 1, 00-601 Warszawa, E-mail: [amni@iem.pw.edu.pl](mailto:amni@iem.pw.edu.pl); dr inż. Jacek Jakubowski, Wojskowa Akademia Techniczna, Instytut Systemów Elektronicznych, ul. Kaliskiego 2, 00-908 Warszawa, E-mail: [jjakubowski@wel.wat.edu.pl](mailto:jjakubowski@wel.wat.edu.pl)